Freckle Formation in Pb-10% Sn Alloy under Various Solidification Conditions

Freckle Formation in Pb-10% Sn Alloy under Various Solidification Conditions

Lisa Philipp[1], Ibrahim Sari[2], Menghuai Wu[1] and Abdellah Kharicha[1,2]

[1] Metallurgy Department, Technical University of Leoben, Franz-Josef-Str. 18, Leoben A-8700, Austria

[2] Christian-Doppler Laboratory for Metallurgical Applications of Magnetohydrodynamics, Technical University of Leoben, Franz-Josef-Str. 18, Leoben A-8700, Austria

[*]E-mail: abdellah.kharicha@unileoben.ac.at

Abstract. Freckles are macrosegregations that form during solidification of alloys. We used a numerical model to study melt and mushy zone behavior under thermosolutal convection and predict freckle formation under various casting conditions. The model simulates fluid flow in a 2D square domain during upward solidification, using a two-phase mixture approach with Boussinesq approximation. The mushy zone is treated as a porous medium with permeability defined by the Carman-Kozeny relation. The aim of the present study is to explore how the effect of temperature gradient and tilted solidification front influences the onset and development of freckles for a Pb-10% Sn alloy. The results indicate delayed freckle formation at higher temperature gradients in a closed cavity under otherwise identical casting conditions. However, a clear correlation between gravity direction and freckle alignment could not be found.

1. Introduction

Freckles are long chains of equiaxed grains that frequently arise in freckle-prone alloys such as tin-lead alloys or Ni-based superalloys during the solidification process. This macrosegregation defect is driven by buoyancy-induced convective flows within the mushy zone, where solute redistribution occurs due to thermosolutal gradients, leading to compositional inconsistencies that degrade material properties and represent a significant obstacle to achieving optimal structural integrity in alloys. Freckles cannot be removed by subsequent thermomechanical treatments, highlighting the critical importance of understanding their formation mechanisms to mitigate their occurrence during alloy production[1][2].

The channel formation process is initiated in the mushy zone - a semi-solid region between fully liquid and solid phases. During solidification, solute rejection occurs as elements with different densities segregate at the solid-liquid interface. Rejected solute concentrates in the liquid phase, resulting in concentration differences across the mushy zone. The temperature gradient as well as the concentration gradient lead to local density variations. Such density gradients become unstable under gravitational force, initiating buoyancy-driven flow known as thermosolutal convection[1][2][3][4][5][6]. Mushy zone permeability is related to dendrite arm spacing and thermal gradient and directly influences the ease of fluid flow, thereby affecting the rate and severity of freckle formation. A higher permeability allows more pronounced fluid flow, leading to increased segregation and defect formation[3][6]. The convective flow leads to instabilities and

channel formation. Thus, segregated liquid is transported from within the mushy zone to the solidification front. Once established, channels are sustained by the local equilibrium between the liquid and solid phases within the mushy zone, with continuous supply of lighter, solute-depleted liquid. Over time, these regions become enriched in solute and form visible defects [1].

This study focuses on freckle formation in a binary hypereutectic Pb-10% Sn alloy considering a linearised phase diagram. The effect of a tilted solidification front on freckle formation was studied, by systematically tilting the gravitational acceleration vector at an angle θ with respect to the vertical direction. Thus, buoyancy force acts in horizontal and vertical direction and simulations were conducted to explore how gravity direction influences the convective flow patterns and resulting channel instabilities within the mushy zone. Additionally, the initial temperature gradient was varied. Freckle formation has been extensively studied under various casting and solidification conditions, mainly for Ni-based superalloys[2][4][11][12]. This study however, explores the combined impact of gravity direction and thermal gradient on freckle onset and alignment in a closed cavity. A number of cases were conducted with $0° \leq \theta \leq 80°$ at initial concentration c_0 = 10 [wt%] Pb.

2. Numerical Model

2.1 Governing Equations

The model employs a two-phase mixture model approach, which significantly reduces computational time and resources. A Boussinesq approximation is utilized, where density ρ is assumed to be constant ($\rho_s = \rho_l = \rho_0$) except in the term for buoyancy force. This simplifies calculations while capturing the essential fluid dynamics driven by temperature and concentration gradients. The velocity of the mixture phase $\vec{u}_m$ is calculated using a weighted average of the liquid and solid phase velocities, with the velocity of the solid phase $\vec{u}_s$ assumed to be zero. c_{mix} denotes the mixture phase concentration and is given by equation (1). f_l and f_s are the liquid and solid fraction, c_l and c_s^* are the liquid and equilibrium solid concentration, respectively. [6]

$$c_{mix} = f_l c_l + f_s c_s^* \tag{1}$$

Table 1. Governing Equations: Mass conservation (2), Momentum conservation (3), Enthalpy conservation (6) and Species conservation (7). [6]

Conservation Equation	
$\frac{\partial \rho_m}{\partial t} + \nabla \cdot (\rho_m \vec{u}_m) = 0$	(2)
$\frac{\partial (\rho_m \vec{u}_m)}{\partial t} + \nabla(\rho_m \vec{u}_m \vec{u}_m) = -\nabla p + \nabla(\mu_m \nabla \vec{u}_m) + \overrightarrow{F_B} + \overrightarrow{F_D} + \nabla \cdot \left(\sum_{i=1}^{2} f_i \rho_i \vec{u}_{dr,i} \vec{u}_{dr,i} \right)$	(3)
$\frac{\partial}{\partial t}(\rho h) + \nabla(\rho_l h_l f_l \vec{u}_l) = \nabla(\lambda_m \nabla T) + Q_s$	(4)
$\frac{\partial (\rho_l f_l c_l)}{\partial t} + \nabla(\rho_l f_l c_l \vec{u}_l) = \nabla(\rho_l D_l \nabla c_l) - \rho_l \left(c_s^* \frac{\partial f_s}{\partial t} + f_s \frac{\partial c_s^*}{\partial t} \right)$	(5)

The continuity equation takes on the form as seen in (2), ρ_m is the density of the mixture phase, respectively. The momentum conservation equation as shown in (3), includes the sum of

the body forces $\vec{F}_i$ that arise from buoyancy and resistance within the mushy zone, in the source term. p and μ are the pressure and viscosity, respectively. The density changes included in the buoyancy term (equation (6)) depend on local temperature and concentration variations, making it the driving force behind thermosolutal convection. $\vec{g}$, β_T and β_c are the gravitational acceleration, thermal expansion coefficient and solutal expansion coefficient, respectively. The thermosolutal buoyancy force is influenced by gravity direction, hence, varying gravitational direction significantly impacts flow patterns within the mushy zone, leading to different channel formation characteristics and freckle distributions. Darcy force is employed using Carman-Kozeny equation in (7), taking into account isotropic permeability of the mushy zone which largely influences solidification and freckle formation. Lower permeability suppresses convective movements, reducing freckle formation likelihood. A_{mush} is the mushy zone constant. The constant ε is set to 10^{-3} and is included to avoid division by zero. [6]

$$\vec{F}_B = \vec{g}\rho(T, c_l)f_l = \vec{g}\rho_0\left[1 - \beta_T\left(T - T_{liq}\right) - \beta_c(c_l - c_0)\right]f_l \quad (6)$$

$$\vec{F}_D = \frac{f_s^2}{(1-f_s)^3+\varepsilon}A_{mush}(\vec{u}_s - \vec{u}_l) \quad (7)$$

Table 2. Thermophysical properties and parameters for Pb-10wt% Sn. [11]

parameters	symbol	value	unit
Initial concentration of Pb	c_0	10	wt%
Liquidus temperature	T_{liq}	492.15	K
Melting temperature of pure Sn	T_m	505.15	K
Partitioning coefficient	k	0.0656	-
Liquidus slope	m	-128.6	K/wt%
Eutectic temperature	T_{eut}	453.15	K
Eutectic concentration	c_{eut}	38.1	wt%
Density	ρ_0	7440	kg/m^3
Thermal expansion coefficient	β_T	6.0*10^{-5}	1/K
Solutal expansion coefficient	β_c	-5.3*10^{-3}	1/(wt%)
Liquid Diffusion coefficient	D_l	4.9*10^{-9}	m^2/s
Mushy zone constant	A_{mush}	10^5	kg/(m^{3}s)
Latent heat	L	5.85*10^4	J/kg
Thermal conductivity	λ	55	W/(mK)
Liquid Viscosity	μ_l	2.47*10^{-3}	Pa s
Specific heat	c_p	260	J/(kgK)

The enthalpy conservation equation (4) accounts for the release of latent heat during solidification, influencing temperature distribution within the domain. c_p, f_i, h_i, λ and Q_s are specific heat capacity, liquid fraction, enthalpy, thermal conductivity of the mixture phase and enthalpy transfer term, respectively. The change in solid fraction over time is derived from the lever rule approach. Species conservation equation for the mixture phase is calculated as seen in equation (5). It considers the exchange of solute between liquid and solid phases, capturing the solute segregation that drives density variations and subsequent convective flows. D_l is the liquid diffusion coefficient. [6]

The present model gives a simplified setup for the modelling of freckle phenomena. [9][10]

2.2 Implementation and parameters

The two-dimensional computational domain is a square closed cavity shown in Figure 1. All boundaries of the computational domain are defined as no-slip walls. A Dirichlet temperature boundary condition is specified exclusively at the bottom boundary, where the bottom wall temperature (T_{bottom}) is maintained below the eutectic temperature (T_{eut}). The left, right, and top boundaries are modeled as adiabatic walls. The domain is initialized with a temperature of 500 [K] and subsequently cooled from the bottom with a fixed temperature, thus, imposing an initial temperature gradient G throughout the computational domain. The effect of two different bottom temperatures $T_{bottom,1}$ = 450 [K] and $T_{bottom,2}$ = 350 [K] that define G_1 = 50 [K] and G_2 = 150 [K], respectively, with angles θ ranging between 0° and 80° were studied. To ensure stability and accuracy a CFL (Courant-Friedrichs-Lewy) criterion was applied. Numerical simulations were implemented using Ansys Fluent 17.1.

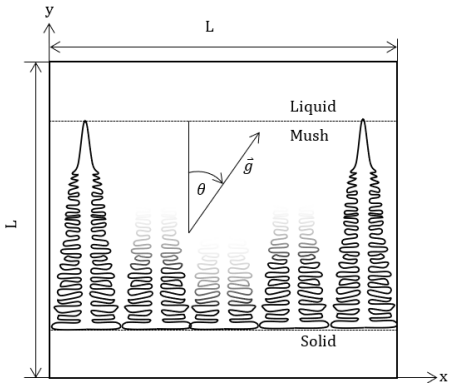

Figure 1. Computational domain with applied boundary conditions. L the domain size[m], $\vec{g}$ the gravitational acceleration [m/s], and θ the inclination angle [°].

3. Results

It has been reported that freckle chains tend to form approximately parallel to gravity direction for a planar interface and at an angle with respect to the vertical plane if the solidification front is tilted. Moreover, the onset of thermosolutal convection in the mushy zone is more likely in the latter case. [7]

Figure 2 depicts a fully solidified freckle distribution under an initial temperature gradient G_1 = 50 [K] at angles 0° < θ < 80°. To improve numerical stability, the angle θ was increased gradually. In each scenario, the onset of channel formation occurs in the lower third of the

computational domain, which defines the critical solidification stage at which thermosolutal convection overcomes the mushy zone's structural resistance. For the case with the gravitational angle set at θ =0° (vertical), the first channels aligned approximately parallel to the gravitational force. The development of these channels indicates strong thermosolutal convection, resulting in significant solute enrichment and therefore, upward liquid movement. Due to interaction between channels that formed in close proximity to each other and the chosen boundary conditions, a rotating flow within the liquid phase ahead of the solidification front formed, as seen in Figure 3. Over time, the channels coalesce, resulting in the formation of larger freckles. The growth direction was strongly impacted by the flow direction within the computational domain. Channels that formed at the upper region of the domain are again aligned with the direction of the gravitational force, as there was insufficient space for the remaining liquid to form a strong flow.

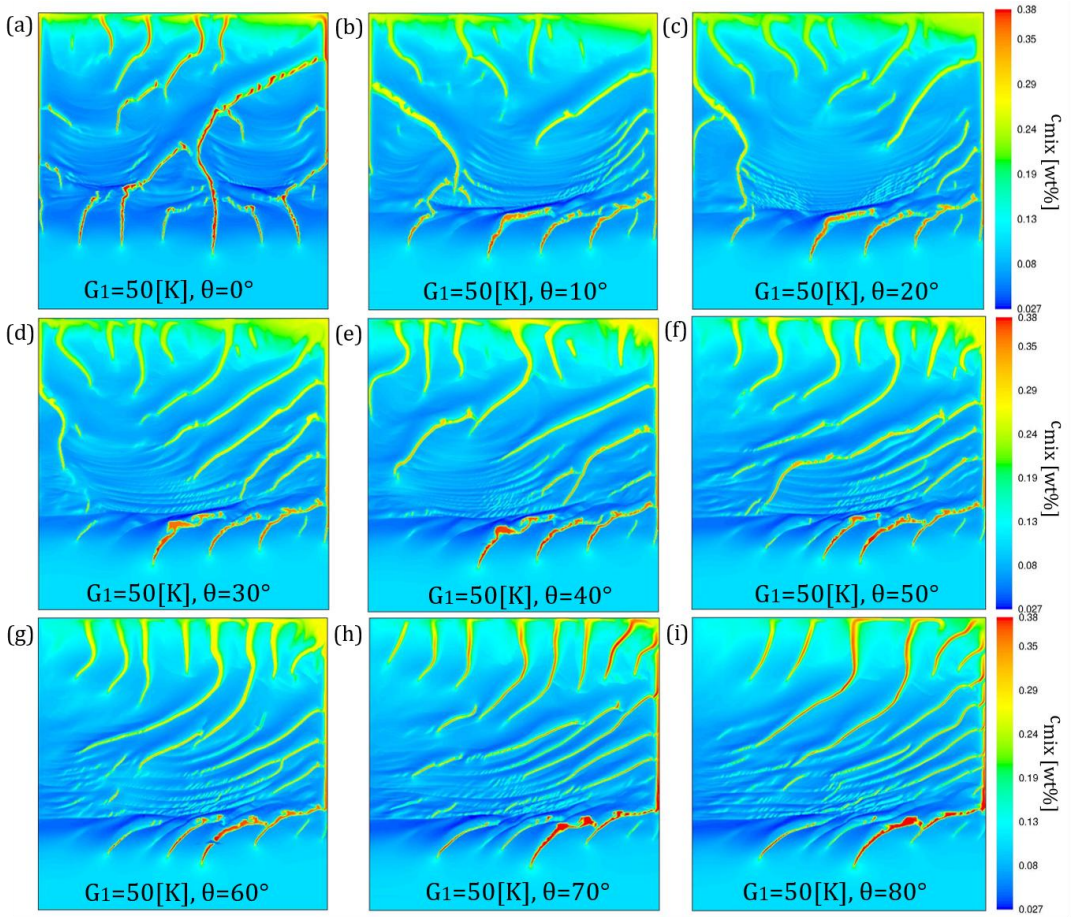

Figure 2. Mixture concentration for G_1 = 50 [K] and θ = 0°(a), θ = 10° (b), θ = 20° (c), θ = 30° (d), θ = 40° (e), θ = 50° (f), θ = 60° (g), θ = 70° (h) and θ = 80° (i).

In the cases where the gravitational angle is set at 10° < θ < 80° (Figure 2(b - i)) with respect to the vertical plane, the channels that form initially lean to the left. This is due to the lateral dragging of the vertical flow from deep within the mushy zone. As a result, freckles in the lower half of the domain form at varying angles with respect to the horizontal plane. The subsequent rotating flow in the liquid phase leads to channel formation similar to the case with vertical

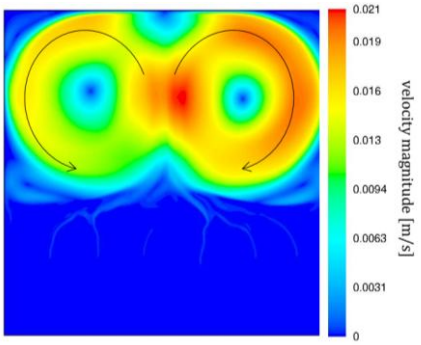

Figure 3. Fluid flow velocity magnitude with indicated flow direction for G_1 = 50 [K] and θ = 0° at time 170 s.

gravity direction. However, in the top region of the domain, the freckles are influenced by the direction of gravity, forming at an angle with respect to the vertical, highlighting the impact of gravity direction in areas without strong flow.

In comparison, Figure 4 illustrates freckle formation under an initial temperature gradient of G_2 = 150 [K], with gravitational angles ranging from 0° to 80°. It is evident that the increased

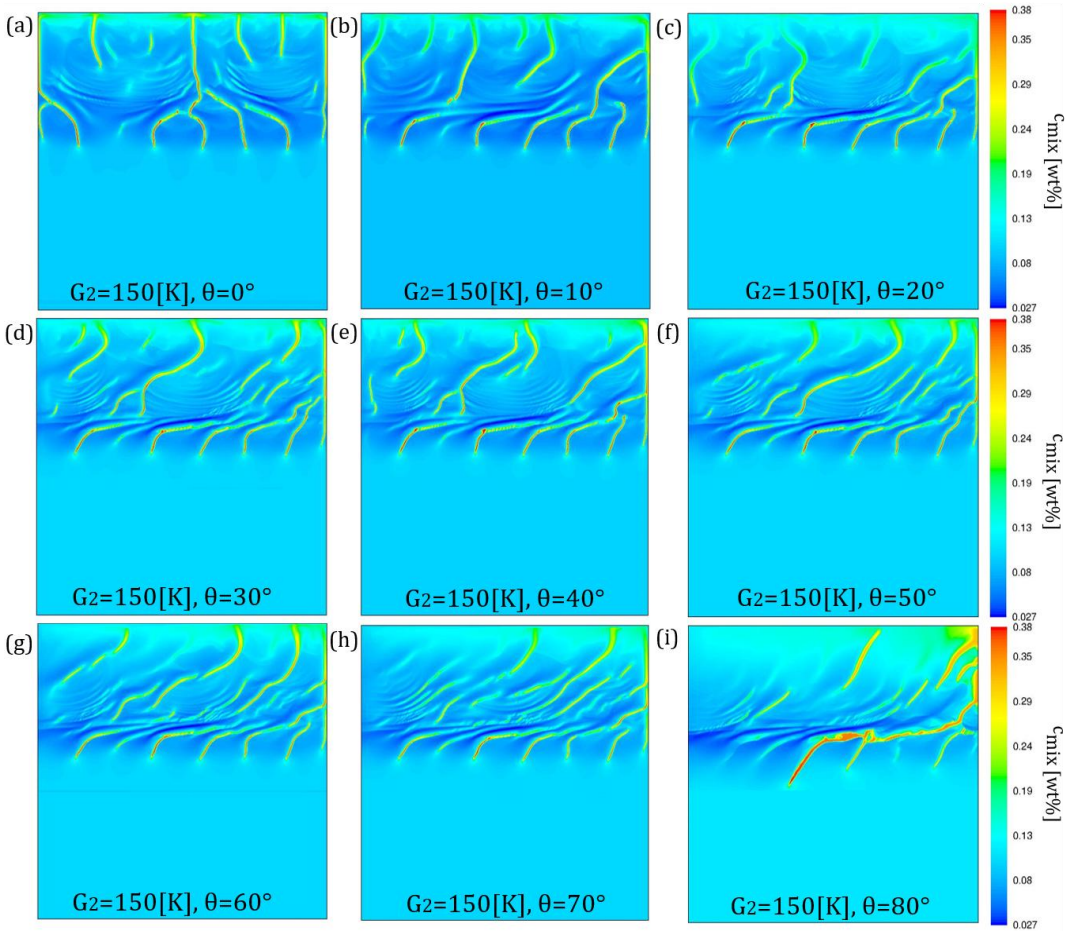

Figure 4. Mixture concentration for G_2 = 150 [K] and θ = 0°(a), θ = 10° (b), θ = 20° (c), θ = 30° (d), θ = 40° (e), θ = 50° (f), θ = 60° (g), θ = 70° (h) and θ = 80° (i).

temperature gradient G_2 influences thermosolutal convection within the domain. Notably, channel initiation occurred significantly later in the upper half of the cell. Although the final freckle distribution resembles that of cases with a temperature gradient of G_1 = 50 [K], the channels formed under the higher temperature gradient G_2 are significantly smaller.

Figure 5 shows the manually measured inclination angles α of freckles at different heights within the computational domain for the two studied initial temperature gradients (G1 = 50 [K] and G2 = 150 [K]) and for various gravitational angles θ. The freckle inclination angle α indicates the direction and degree of tilt of the freckles relative to vertical alignment. Positive values represent a tilt to the right, whereas negative values indicate a tilt to the left. It is evident that at a lower initial temperature gradient G_1, freckles form across a broader height range within the domain and tend to incline consistently towards the right as the gravitational angle θ increases. Near the top of the domain alignment again varies. Conversely, a higher temperature gradient G_2 delays the onset of freckle formation, causing freckles to form higher in the domain. This observation is supported by the findings of Schneider et.al. for directional solidification of Ni-based superalloys [12]. At an increased temperature gradient, freckles in the present work display generally slightly smaller inclination angles. Overall, the results of the study show that while the direction of gravitational forces influence the initial channel formation, they do not significantly affect the onset of channel formation and final freckle distribution. In contrast, the rotating flow within the liquid phase plays a much stronger role in shaping the freckle patterns. When the gravitational angle is tilted, channels initially form at an angle to the horizontal plane due to lateral flow in the mushy zone. These findings emphasize that the gravity direction influences the early and late stages of solidification. However, it is the rotating liquid flow driven by buoyancy in the purely liquid region that ultimately dictates the freckle distribution in the final solidified structure.

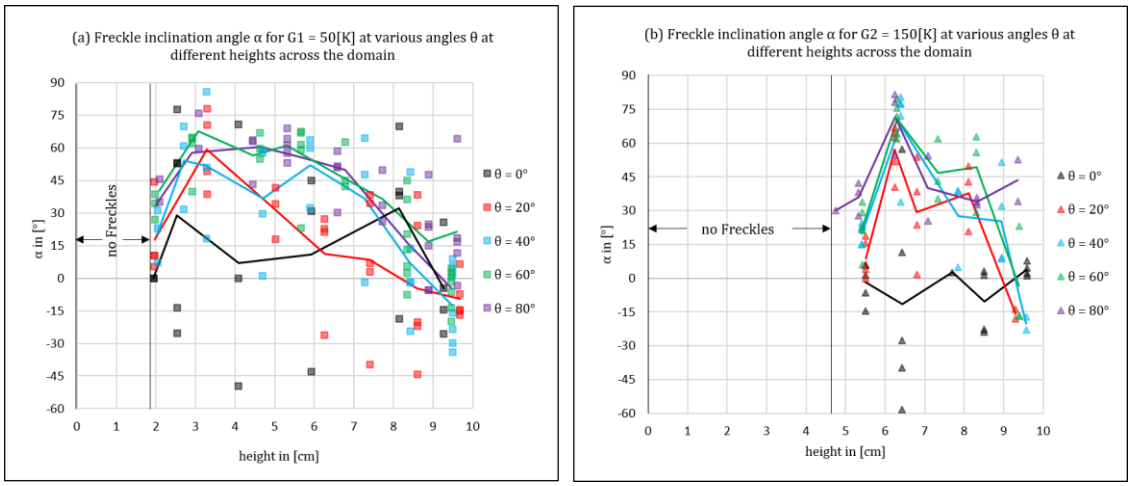

Figure 5. Freckle inclination angles α for (a) $G_1$and (b) G_2 for various angles θ, measured at different domain heights. Lines refer to the average inclination angle at each domain height.

4. Conclusion

In this study, we developed a numerical model to explore freckle formation in a binary Pb-Sn alloy during varying solidification conditions in a closed cavity, considering both vertical and tilted

solidification fronts. The model captures complex interactions between gravity direction, solute concentration and thermal conditions, providing a comprehensive understanding of the factors influencing freckle formation. The results of the simulations demonstrate how changes in solidification conditions influence the onset and development of freckle formation. Our findings suggest that tilted solidification fronts influence the initial and final channel formation. However, this does not significantly alter the final freckle distribution. Instead, the rotating flow in the liquid phase plays a much more significant role in shaping the final freckle patterns. Additionally, we observed that an increased initial temperature gradient (G_2 = 150 [K]) delays the onset of channel formation and leads to narrower channels compared to lower initial temperature gradient (G_1 = 50 [K]). These results underline the critical role of thermosolutal convection and the dynamics of liquid flow in controlling freckle formation, offering valuable insights for optimizing solidification conditions and minimizing defects in alloy casting.

Acknowledgments

The authors acknowledge financial support by the Austrian Federal Ministry of Economy, Family and Youth and the National Foundation for Research, Technology and Development within the framework of the Christian-Doppler Laboratory for Metallurgical Applications of Magnetohydrodynamics.

References

[1] Kao, A., Shevchenko, N., Alexandrakis, M., Krastins, I., Eckert, S., Pericleous, K. Thermal dependence of large-scale freckle defect formation. Philosophical transactions. Series A, Mathematical, physical, and engineering sciences. (2019).

[2] Auburtin, P. Determination of the Influence of Growth Front Angle on the Freckle Formation in Superalloys, PhD Thesis, University of British Columbia, Canada. (1998)

[3] Ramirez, J.C., Beckermann, C. Evaluation of a rayleigh-number-based freckle criterion for Pb-Sn alloys and Ni-base superalloys. Metall Mater Trans A 34, 1525–1536 (2003).

[4] Ma, D., Zhou, B., Bührig-Polaczek, A. Investigation of Freckle Formation under Various Solidification Conditions. Advanced Materials Research. (2011).

[5] Beckermann, C., Gu, J.P. & Boettinger, W.J. Development of a freckle predictor via rayleigh number method for single-crystal nickel-base superalloy castings. Metall Mater Trans A 31, 2545–2557 (2000).

[6] Sari, I., Wu, M., Ahmadein, M., Ataya, S., Alrasheedi, N., Kharicha, A. The Impact of Marangoni and Buoyancy Convections on Flow and Segregation Patterns during the Solidification of Fe-0.82wt%C Steel. Materials. 2024.

[7] Zhang, Y., Chen, W., Chen, L., Yan, Q., Zhang, Y. Evaluating tendency of freckle formation for electro-slag remelting 20SiMn2MoV ingots by experiments and simulation. Metallurgical Research & Technology. 111. 259-269, (2014).

[8] Copley, S.M., Giamei, A.F., Johnson, S.M. *et al.* The origin of freckles in unidirectionally solidified castings. *Metall Trans* **1**, 2193–2204 (1970).

[9] Wu, M., Kharicha, A., Ludwig, A. (2014). Numerical Study of the Influence of Diffusion-Governed Growth Kinetics of Ternary Alloy on Macrosegregation. Materials Science Forum. 790-791. 85-90, (2014).

[10] Wu, M.,Li, J., Ludwig, A., Kharicha, A. Modeling diffusion-governed solidification of ternary alloys – Part 2: Macroscopic transport phenomena and macrosegregation, Computational Materials Science, Volume 92, 267-285,(2014).

[11] Zhang, Z., Wu, M., Zhang, H., Karimi-Sibaki, E., Ludwig, A., Kharicha, A. (2020). Modeling mixed columnar-equiaxed solidification of Sn-10wt%Pb alloy under forced convection driven by travelling magnetic stirring. IOP Conference Series: Materials Science and Engineering. 861, (2024).

[12] Schneider, M.C., Gu, J.P., Beckermann, C. *et al.* Modeling of micro- and macrosegregation and freckle formation in single-crystal nickel-base superalloy directional solidification. *Metall Mater Trans A* 28, 1517–1531 (1997).